



HAL
open science

A liquid to amorphous transition in Cu-Zr diffusion couples at low cooling rate from chemically constrained liquid

Julien Zollinger, D. Aboudi, S. Migot, J. Ghanbaja

► **To cite this version:**

Julien Zollinger, D. Aboudi, S. Migot, J. Ghanbaja. A liquid to amorphous transition in Cu-Zr diffusion couples at low cooling rate from chemically constrained liquid. *Journal of Non-Crystalline Solids*, 2022, 590, pp.121672. 10.1016/j.jnoncrysol.2022.121672 . hal-03798204

HAL Id: hal-03798204

<https://hal.univ-lorraine.fr/hal-03798204v1>

Submitted on 5 Oct 2022

HAL is a multi-disciplinary open access archive for the deposit and dissemination of scientific research documents, whether they are published or not. The documents may come from teaching and research institutions in France or abroad, or from public or private research centers.

L'archive ouverte pluridisciplinaire **HAL**, est destinée au dépôt et à la diffusion de documents scientifiques de niveau recherche, publiés ou non, émanant des établissements d'enseignement et de recherche français ou étrangers, des laboratoires publics ou privés.

A liquid to amorphous transition in Cu-Zr diffusion couples at low cooling rate from chemically constrained liquid

J. Zollinger^{a,b,*}, D. Aboudi^{a,c}, S. Migot^a, J. Ghanbaja^a

^aUniversité de Lorraine, Institut Jean Lamour, Department of Metallurgy & Materials Science and Engineering, Campus ARTEM, Allée André Guinier, F-54011 Nancy, France.

^bLaboratory of Excellence on Design of Alloy Metals for low-mAss Structures ('LabEx DAMAS'), France

^cDept. SDM, FGMGP, Université des Sciences et de la Technologie Houari Boumediene, 16000, Algiers, Algeria.

Abstract

Amorphous layer up to 20 μm thick were obtained from bulk diffusion couples between pure copper and Zircaloy₄ after isothermal treatment at 900°C and slow cooling to room temperature. It has been shown that the Cu-rich liquid exhibit a low mobility and high viscosity, and that the asymmetrical diffusion behavior of Zr and Cu together with the interfacial reaction rate constrain the liquid layer and allows to avoid nucleation of intermetallic compounds up to 45 minutes holding time. The Cu-rich liquid layer forming at the holding temperature is stable and grows until another liquid, richer in Zr, appears.

Keywords: Amorphous alloys, Cu-Zr system, diffusion, phase transformation

1. Introduction

The first metallic glasses were obtained by rapid quenching of the melt with cooling rates of the order of 10^6 K.s^{-1} [1]. The critical cooling rate leading to an amorphous phase from the melt have been substantially lowered down to 0.1 K.s^{-1} by stabilising the liquid phase through alloy compositions, forming bulk metallic glasses [2]. A simple binary system leading to the formation of bulk glassy alloy is the Cu-Zr system [3]. The usual glass formation range for these alloys is ranging from ≈ 35 to 60 at.% Zr for samples obtained from the melt [4]. Interestingly, the Cu-Zr system is also one of the first reported metallic glass forming system that can produce an amorphous phase from solid-state processes when annealing multi-layer thin films [5]. In that case the glass phase obtained is Cu-rich (20 at.% Zr) [6].

In a previous paper the authors studied the joining of stainless steel to Zircaloy₄ with a copper interlayer by diffusion bonding [7]. At 900°C holding temperature for 45 minutes, the solid layer which formed was expected to be the intermetallic phase $\text{Cu}_{51}\text{Zr}_{14}$ from the stoichiometry deduced from chemical analysis. In this paper, supported by new experiments, it is shown that the layer is composed of an amorphous phase that forms during cooling of the samples.

It is demonstrated that the liquid to glass transition at a micron scale is possible in a narrow heat treatment temperature range where the diffusion rate competes with nucleation events at the bcc-Zr interface. To the knowledge of the authors, this is the first liquid to glass transition formed in a bulk diffusion couple.

2. Materials and methods

Cylindrical bars of Zircaloy₄ (Zr-1.07Sn-0.35Fe, in at.%) with dimensions $\varnothing 8 \times 7 \text{ mm}$ were heat treated with a copper interlayer of 500 μm (grain size 10 μm) thick disk in a graphite cell. Such assemblies were treated under high purity argon flux after a primary vacuum of 10^{-3} mbar was established, at temperatures of 600 and 900°C and holding times of 0, 15 and 45 minutes. A dynamic uniaxial load was applied to ensure good contact between the different materials, decreasing linearly from 29 MPa to 0 MPa once the treatment temperature was reached. After holding, the samples were cooled at 20 K.min^{-1} to room temperature. SEM BSE images and EDS analyses were performed on a FEI Quanta 600 F FEG-SEM equipped with a Brücker Si-drift Quantax EDS detector. Lamella foils for TEM examination were prepared using a focused ion beam (FIB)-SEM dual beam system (FEI Helios NanoLab 600i) using the 'in-situ' lift-out technique. Transmission electron microscopy (TEM) investigations were carried out using a JEOL - ARM 200F Cold FEG TEM/STEM operating at 200 kV and equipped with a spherical aberration (Cs) probe and image correctors (point resolution 0.12 nm in TEM mode and 0.078 nm in STEM mode).

Gibbs free energy for the different phases and compounds of the Cu-Zr system were calculated using the ThermoCalc software [8] and the thermodynamic description of Abe *et al.* [9]. This latter description includes a thermodynamic model for the glass transition initially proposed by Shao [10]. In this model, the glass transition is considered as a second order transition, and the molar free energy change associated to the glass transition is described using:

$$\Delta G_m^{\ell-Am} = -RT_g \ln(1 + \alpha) f(\tau) \quad (1)$$

*Corresponding author.

Email address: julien.zollinger@univ-lorraine.fr

where T_g is the glass transition temperature, α is a factor related to amorphization, τ is the temperature normalised by T_g and $f(\tau)$ is a Hillert-Jarl function [11]. The thermodynamic description also describe the short range ordering in the liquid phase using the associated solution model. A single associate in the liquid phase with the stoichiometry Cu_2Zr is used, corresponding to the minimum of the liquid mixing enthalpy found for this composition [12]. The Gibbs free energies of the solid phases are calculated with the description by Zaitsev and Zaitseva [13].

3. Results

Figure 1 shows the interfacial region of the diffusion couple held for 45 minutes at 900°C , going from copper to Zircaloy₄, bottom to top respectively. Above the copper layer is a solid phase layer of $20\ \mu\text{m}$ later identified as amorphous (see Figure 2). Above is another layer of intermetallic compounds (IMC) that is thought to be liquid at the treatment temperature. Its lenticular shape is typical of surface and grain boundary wetting by a liquid phase. In this sample the IMC layer thickness varies from $2\ \mu\text{m}$ when in the form of a very thin layer to $50\ \mu\text{m}$ when having a lenticular shape. The IMC layer contains 56 at.% Zr and is mainly composed of CuZr_2 with precipitates of CuZr and $\text{Cu}_{10}\text{Zr}_7$, identified by TEM. In contact with the IMC layer is the Zircaloy₄; a diffusion affected zone of approximately $200\ \mu\text{m}$ is also visible in Figure 1. No reaction occurred at 600°C regardless of the holding times investigated. At 900°C , after 0 minutes, an amorphous reaction layer of $1\ \mu\text{m}$ was observed and the amorphous layer was $10.6\ \mu\text{m}$ after 15 minutes of holding. No IMC layer was observed for these two treatments.

Figure 2(a) shows a bright-field low magnification TEM image of the copper / reaction layer interface, and the insert shows the selected area electron diffraction (SAED) pattern corresponding to the red dot circle in the Figure, indicating the amorphous nature of the reaction layer. Figure 2(b) shows a bright-field TEM image of the copper (top left) / reaction layer (bottom right) interface. The interface is faceted with visible steps, and facets are mainly following the $\langle 111 \rangle$ closed-pack

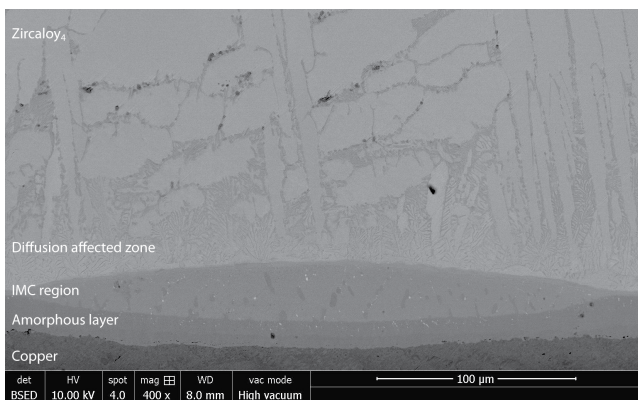


Figure 1: SEM-BSE overview of the microstructure of the Cu-Zircaloy₄ reaction layer after 45 min. at 900°C .

planes. Figure 2(c) shows the same interface at higher resolution with the corresponding FFTs patterns in small inserts. These figures clearly show the crystalline copper in contact with an amorphous phase, as revealed by the typical "orange-peel" aspect of the microstructure and by the SAED pattern.

Figure 3(a) shows the evolution of the Zr content from pure copper to Zircaloy₄ in a couple held 45 min. at 900°C in a region where the IMC layer is only a few microns thick. The amorphous layer has a limited composition range around 21 at.% Zr, with a minimum at the copper interface of 18.8 at.% and a maximum value of 22.4 at.% at the IMC/Zircaloy₄ interface. For the different holding times investigated, these values evolve poorly and remain in the uncertainty associated with the measurement, *i.e.* $\pm 0.5\text{at.}\%$. Within this composition range and in between room temperature and 900°C , four IMCs can possibly form *i.e.* Cu_9Zr_2 , $\text{Cu}_{51}\text{Zr}_{14}$, Cu_8Zr_3 and $\text{Cu}_{10}\text{Zr}_7$. Figure 3(b) show the amorphous layer thickness evolution with time compared with the calculated thickness for the stable IMC phases having a stoichiometry close to the liquid composition and the liquid phase with diffusion and growth data found in the literature. The data for the liquid was taken from [14]. The growth rate of the IMC was taken from ref. [15]. The experimental data was fitted assuming a parabolic growth, such that the thickness of the layer $d = k.t^{1/2}$ where k is a rate constant dependent on the diffusion coefficient and t the time. The good agreement between the exp. data and the fitting curves shows that the growth is limited by volume diffusion. At this temperature and composition, the layer is expected to be liquid but as can be seen from Fig. 3(b), the layer grows much slower than expected for the liquid phase.

Using the concentration profiles as in Figure 3(a) the inter-diffusion coefficient of Zr can be estimated using the Heumann's method [16] by making the assumptions that the composition evolves linearly within the layer and that the inter-diffusion coefficient is not dependent of the Zr content. This leads to an average value of $D_{\text{Zr}} = 2.21 \pm 0.25 \times 10^{-11}\ \text{m}^2/\text{s}$ which is a surprisingly low value for a liquid phase. The dynamic viscosity can be deduced from the Stokes-Einstein relationship:

$$\eta = \frac{k_B T}{6\pi D_{\text{Zr}} r_{\text{Zr}}} \quad (2)$$

where k_B is the Boltzmann constant, and r_{Zr} is the ionic radius of zirconium. This equation leads to the viscosity value of $540\ \text{mPa}\cdot\text{s}^{-1}$ which is a relatively high value even compared to results given for a Cu-60Zr liquid alloy of $92\ \text{mPa}\cdot\text{s}^{-1}$ at the same temperature of 900°C [9]. It has to be mentioned that the IMC layer that is expected to be liquid at 900°C has a composition ranging from 45 to 50 at.% Zr. For the average composition of 21 at.% Zr of the amorphous layer at 900°C , it can be seen from the equilibrium phase diagram in Figure 4(a) that the liquid is substantially undercooled since for this composition the $\text{Cu}_{51}\text{Zr}_{14}$ compound melt congruently at 1160°C . This high viscosity can also explain the very faceted copper / amorphous interface shown in Fig. 2(a) while a rough solid/liquid interface is usually expected at solid/liquid interfaces in metallic alloys.

After 45 min at 900°C , two liquids having different compositions are in contact and only the copper-rich liquid will be

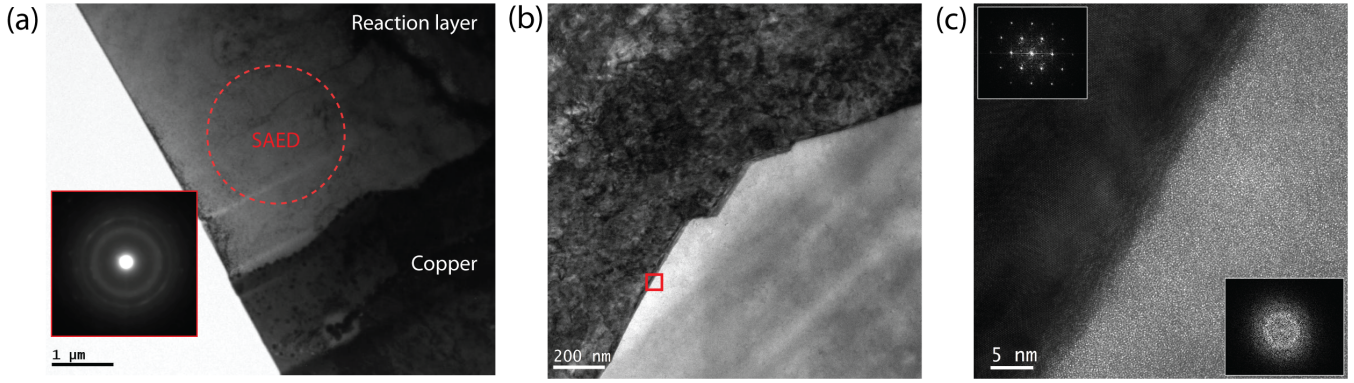


Figure 2: (a) Bright-field low magnification TEM image of the copper / reaction layer interface, the insert shows the SAED pattern taken from the red dot circle, (b) bright-field TEM micrograph of crystalline copper (top left) / amorphous layer (bottom right) interface. (b) HRTEM micrograph in area indicated by a red square, inserts in (c) are the fast Fourier transforms calculated in the crystallized zone and in the amorphous zone.

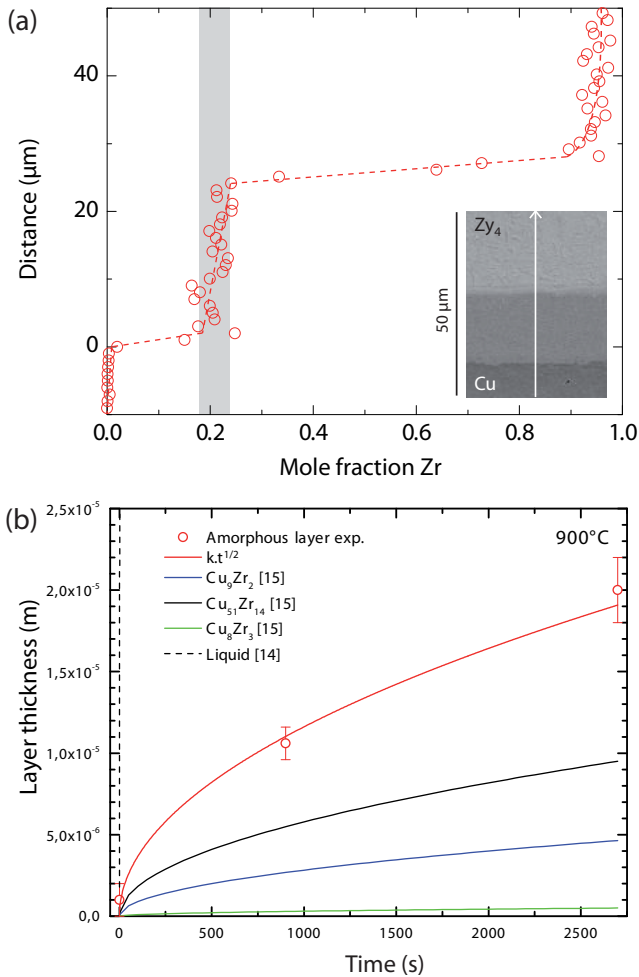


Figure 3: (a) Composition profile in zirconium from copper to Zircaloy measured by EDS (SEM). The greyed area corresponds to the solid layer composition range. The holding temperature is 900°C. (b) Layer thickness evolution with time for the phases likely to form in the composition range investigated at 900°C. Data is taken from [14] for the liquid phase and from [15] for the intermetallics compounds.

come amorphous. Thermodynamic calculations were made to determine the metastable Cu-Zr phase diagram that is presented in Figure 4(b) with solid solutions and liquid phase only. In this Figure, the red rectangle shows the usual range of amorphous alloys which are produced by melt quenching and the grey rectangle indicates the composition range found in this paper. The red dashed line indicates the glass transition temperatures. Due to the amorphous layer thickness it was not possible to determine the glass transition temperature, but amorphous Cu-Zr alloy produced by low temperature solid-state reaction and having similar composition has a $T_g = 703 \text{ K}$ (430 °C) [6]. The unknown univariant type reaction $\text{Cu} + \text{Liq. 1} \rightarrow \text{Liq. 2}$ occurs because of the minimum of the liquid mixing enthalpy found at 33 at.% Zr [12] and implemented in the Gibbs free energy description of the liquid phase.

4. Discussion

The formation of up to 20 μm thick amorphous layer from a Cu-20%Zr liquid at low cooling rate was observed. This region of the system is, for liquid to amorphous transition, much less characterised than compositions richer in Zr [17]. Cu-20%Zr quenched from the liquid usually leads to the formation of intermetallic glasses [18]. In the present work, the amorphous transition is possible if no IMC nucleate during the diffusion process, despite long isothermal holding. It can be explained by the dynamic stability of the liquid film during the holding, constrained to each of its interfaces. At the interface with copper, the chemical gradient is very sharp because Zr is a slow diffuser in Cu [19], such that the liquid / Cu interface velocity remains faster than the diffusion velocity of Zr in Cu. Moreover, sharp chemical gradients at the interface increase the work for cluster formation, thus inhibiting nucleation [20, 21]. At the interface with Zr, since diffusion of Cu is very slow in the liquid layer and very fast in the Zr, the layer probably grows faster at this interface. The interfacial reaction is then faster than the enrichment of Cu in Zr. The amorphous layer stops to grow when the Zr-rich liquid appears, probably when the diffusion profile of Cu in Zr flattens leading to the IMC region in Figure 1. These features

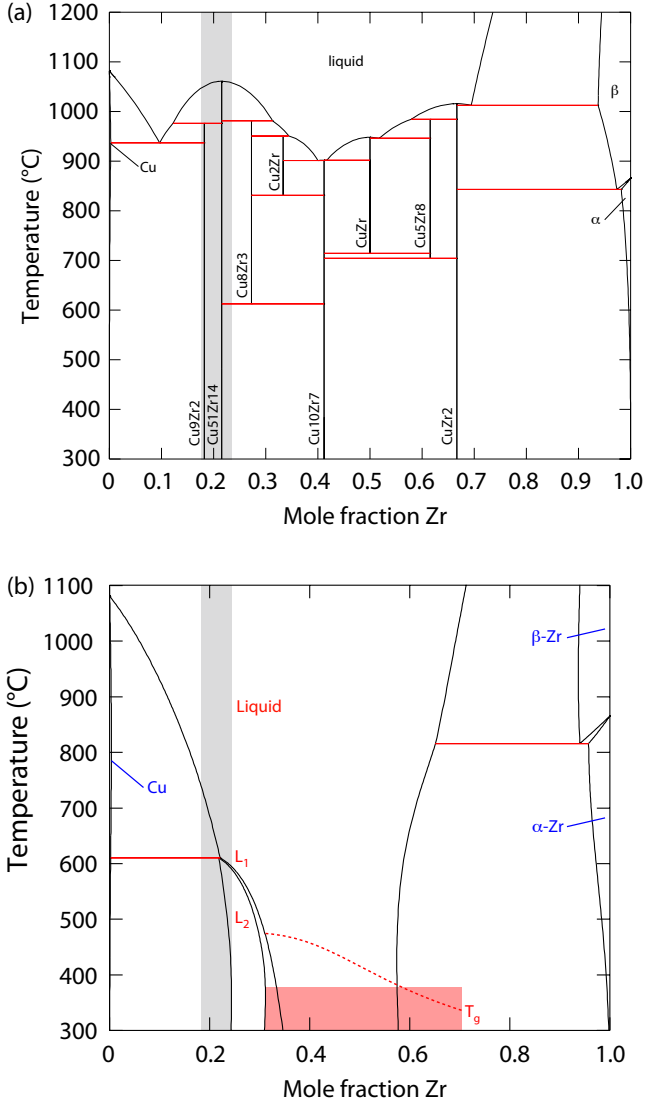


Figure 4: (a) Equilibrium Cu-Zr phase diagram. (b) Calculated metastable binary phase diagram with solid solutions and liquid only. The greyed area corresponds to the amorphous layer composition. The red rectangle indicates the usual binary amorphous alloys composition range and the red dashed line the corresponding glass transition. Note the two peculiar univariant reactions: (i) metatectic $\beta\text{-Zr} \rightarrow \text{Liq.} + \alpha\text{-Zr}$ and (ii) unknown univariant type $\text{Cu} + \text{Liq.} 1 \rightarrow \text{Liq.} 2$.

are illustrated schematically in Figure 5. Finally, IMC could homogeneously nucleate directly from the liquid layer but it has not been observed either. Considering the classical nucleation theory from the liquid phase, the nucleation rate I of a phase is given by $I = I_0 \cdot \exp(-W^*/kT)$. The pre-exponential term I_0 is proportional to the diffusion coefficient in the liquid; the low value of this coefficient determined in this work. Moreover the critical work for cluster formation, W^* , increases with the cubic power of the interfacial energy, $\gamma_{s/\ell}$. As shown by Hoyt et al. in the Cu-rich side of the Cu-Zr system, the interfacial energy increases strongly when the liquid is highly undercooled [22], close to the 260 K reached in this study. With the influence on I_0 and W^* (through $\gamma_{s/\ell}$), the nucleation rate should

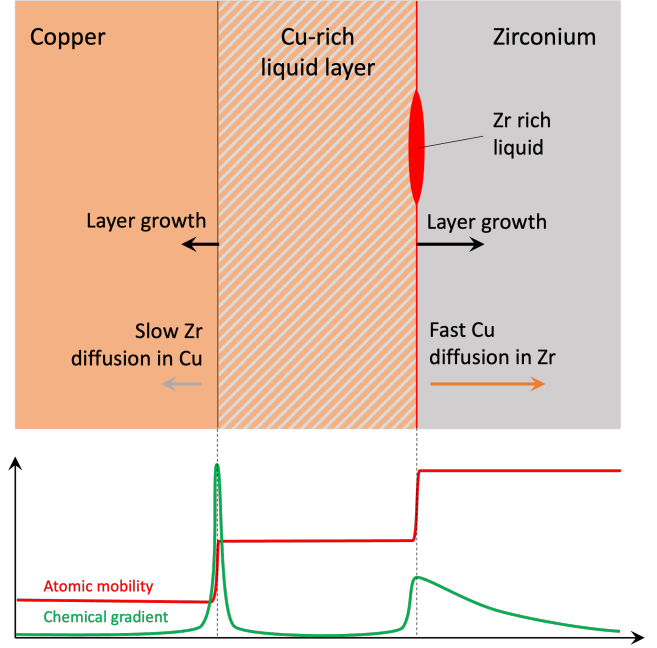


Figure 5: Schematics of the Cu-rich liquid formation leading to amorphous after cooling from 900°C. Zr rich liquid was observed after 45 minutes holding time. Qualitative evolution of the atomic mobility and chemical gradients along the layers is also represented.

be drastically decreased in the liquid layer. A final remark concerns the role of oxygen, since Zr is a reactive element in particular with oxygen, and that this element has a strong effect on the glass forming ability in Zr containing metallic glasses [23]. EDS in TEM showed an oxygen content less than 0.4 at.% in the amorphous layer, while a larger amount was found in the liquid phase which is richer in Zr in which intermetallic compounds form upon cooling (oxygen contents ranging between 0.7 to 4 at.%). Further experiments will be carried out in order to limit the oxygen pick-up during thermal processing and to investigate its influence on the results presented here.

5. Conclusions

The formation of micro-metric layer of amorphous Cu-20%Zr from bulk diffusion couples has been reported. The amorphous layer forms at slow cooling rate, which is unusual even for the Cu-Zr system. We have shown that it is due to a liquid with low mobility, constrained at Cu and Zr interfaces by the competition between asymmetrical diffusion rate and interface mobility. The layer stops growing when a Zr-rich liquid starts to grow at the Zr interface.

Acknowledgements

J.Z. would like to thank Dr. G. Kurtuldu and Pr. A.L. Greer for their enlightened comments on this manuscript. This work was supported by the Algerian Ministry of Higher Education and Research (267/PNE/ENS/2015-2016) and by the French National Research Agency (ANR) referenced by ANR-11-LABX-0008-01.

References

- [1] W. K. Jun, R. Willens, P. Duwez, *Nature* 187 (1960) 869.
- [2] A. Inoue, *Acta Mater.* 48 (2000) 279–306.
- [3] A. Inoue, W. Zhang, *Mater. Trans.* 45 (2004) 584–587.
- [4] O. J. Kwon, Y. C. Kim, K. B. Kim, Y. K. Lee, E. Fleury, *Met. Mater. Int.* 12 (2006) 207–212.
- [5] M. Atzmon, J. D. Verhoeven, E. D. Gibson, W. L. Johnson, *Appl. Phys. Lett.* 45 (1984) 1052–1053.
- [6] K. Bhanumurthy, G. K. Dey, S. Banerjee, *Scripta Metal.* 22 (1988) 1395–1398.
- [7] D. Aboudi, S. Lebaili, M. Taouinet, J. Zollinger, *Mater. Des.* 116 (2017) 386–394.
- [8] J. Andersson, T. Helander, L. Höglund, P. Shi, B. Sundman, *Calphad* 26 (2002) 273–312.
- [9] T. Abe, M. Shimono, M. Ode, H. Onodera, *Acta Mater.* 54 (2006) 909–915.
- [10] G. Shao, *J. Appl. Phys.* 88 (2000) 4443–4445.
- [11] M. Hillert, M. Jarl, *Calphad* 2 (1978) 227–238.
- [12] O. Kleppa, S. Watanabe, *Metal. Trans. B* 13 (1982) 391–401.
- [13] A. Zaitsev, N. Zaitseva, *High Temp.* 41 (2003) 42–48.
- [14] M. Mendeleev, M. Kramer, R. Ott, D. Sordelet, *Phil. Mag.* 89 (2009) 109–126.
- [15] O. Taguchi, Y. Iijima, K. Hirano, *J. Alloys Compd.* 215 (1994) 329–337.
- [16] T. Heumann, *Z. Phys. Chem.* 201 (1952) 168–189.
- [17] R. Yuan, Z. Yu, H. Leng, K. Chou, *J. Non-Cryst. Solids* 564 (2021) 120835.
- [18] Y. Wang, J. Yao, Y. Li, *J. Mater. Sci. Technol.* 34 (2018) 605–612.
- [19] A. Greer, N. Karpe, J. Böttiger, *J. Alloys Compd.* 194 (1993) 199–211.
- [20] P. Desre, A. Yavari, *Phys. Rev. Lett.* 64 (1990) 1533.
- [21] S. Q. Arlington, F. Yi, D. A. LaVan, T. P. Weihs, *AIP Advances* 9 (2019) 035324.
- [22] J. Hoyt, S. Raman, N. Ma, M. Asta, *Comp. Mat. Sci.* 154 (2018) 303–308.
- [23] W. H. Wang, *Prog. Mater. Sci.* 52 (2007) 540–596.